*International Journal of Fracture* **109:** 263–283, 2001.


# Interactions of fatigue cracks with elastic obstacles

C. H. WANG[1] and J. W. HUTCHINSON[2]
[1]*Aeronautical and Maritime Research Laboratory, Defence Science and Technology Organisation, 506 Lorimer Street, Fishermans Bend, VIC 3207, Australia*
[2]*Division of Engineering and Applied Science, Harvard University, Cambridge, MA 02138, USA*

Received 10 May 2000; accepted in revised form 17 November 2000

**Abstract.** To quantify the growth behaviour of fatigue cracks growing towards microstructural barriers or elastic obstacles, parametric solutions are obtained for crack-tip opening displacement and plasticity-induced crack closure of a mode I fatigue crack growing towards elastic obstacles. Three common bi-material systems are analysed using the finite element method, in which both constituent materials have identical elastic properties but only the phase that contains the crack can deform plastically. It has been found that under monotonic loading the crack-tip opening displacement decreases as the crack-tip approaches the interface boundary, but reaching a non-zero value when the crack-tip terminates at the boundary. For a fatigue crack growing under constant amplitude loading, the crack-closure stress has been found to increase as the crack grows towards the barrier. Based on these results a mechanistic model is proposed to quantify the influence of stress level on the fatigue threshold of microstructurally small fatigue cracks, with predictions being in close agreement with experimental data.

**Key words:** Blocked-slip model, crack-tip opening displacement, dugdale model, elastic obstacles, fatigue crack closure, fatigue limit, large-scale yielding, microstructural barrier, small fatigue cracks.

## 1. Introduction

The propagation of fatigue cracks whose size is on the order of the microstructure has been found to be strongly dependent on the crack-microstructure interactions, with stress-state and amplitude also affecting such interactions (Miller, 1993; McDowell, 1996; Liu, 1998, 1999). Examples of microstructural barriers to crack growth include grain boundaries, twin boundaries, and hard particles or phases with higher yield strength. Such interactions have been identified as the primary mechanism responsible for the observed oscillatory behaviour of microstructurally short cracks. For instance, under constant amplitude loading conditions, a distinguishing feature of microstructurally short crack propagation is the deceleration with crack length or even arrest upon encountering an obstacle or microstructural barrier (Miller, 1991). Experimental studies have confirmed the existence of non-propagating cracks, with length comparable to the typical grain dimension, at stress levels below the fatigue limit (Miller, 1993). These findings suggest that fatigue damage can be related to the growth of fatigue cracks, and fatigue resistance can be equated to the limiting conditions for the propagation a crack. Consequently it should be possible to develop a mechanistic approach which can quantify the growth behaviour of fatigue cracks from the micro-scale to the macro-scale and to the large-scale. Two major challenges facing the development of such a unified approach which can link the scales in fatigue crack propagation are (i) to identify a consistent correlating parameter suitable across these different scales, and (ii) to quantify the interactions of fatigue cracks with microstructure.

The interactions between cracks and a material's texture are affected by many aspects of the material's microstructure, such as crystallographic orientations, the size and shape of grains, the size and distributions of second phases and inclusions, and material heterogeneity and anisotropy. Several distributed dislocation theory-based approaches have been developed to simulate the blocking effect of grain boundaries on the growth of short cracks (Tanaka et al., 1986; Navarro and de los Rios, 1987, 1988). Although these models are most appropriate for shear mode crack growth, they have been applied to deal with tensile mode crack growth, by appealing to the Dugdale model for plane stress. One distinct feature of these dislocation-theory based models is that the crack-tip opening displacement (CTOD) is predicted to decrease to zero as the crack-tip approaches a grain boundary, assuming no plastic deformation would occur in the next grain (Navarro and de los Rios, 1987, 1988). While these models have shown some success in simulating the observed oscillatory pattern of short crack growth rates, these models are strictly speaking applicable to only shear mode cracks. It is unlikely that the assumption of strip yielding is valid for tensile cracks, especially under plane strain conditions. This decreasing trend in CTOD has been confirmed by a finite element analysis of an edge crack in a bi-material structure consisting of a perfectly plastic single crystal and an elastic solid (Hutchinson and Tvergaard, 1999). However, it is not clear from these results whether CTOD would actually decrease to zero as the crack-tip approaches the boundary.

By employing the finite element method, Hutchinson and Tvergaard (1999) obtained some basic solutions of the crack-tip sliding and opening displacement of edge cracks in single crystals under cyclic loads. Results were obtained assuming that the crystal itself does not experience overall yielding, and there is no crack face contact. The preliminary results suggested that the crack-tip opening and sliding displacements decrease as the crack tip approaches a grain boundary across which the crystallographic orientation changes, consistent to the trend expected from the distributed dislocation theory-based approaches. It was noted by Hutchinson and Tvergaard (1999) that several important issues are yet to be resolved. Firstly, quantitative results for the interactions under cyclic loading are required to understand the condition under which crack arrest by obstacles or barriers would occur. Second, solutions pertaining to large-scale yielding or gross-section yielding are essential to the development of quantitative methods. This is because for fatigue crack nucleation to occur in a polycrystal, extensive plasticity relative to the crack size may invalidate the applicability of small-scale yielding solutions. In some cases a small fraction of surface crystals favourably oriented for slip may even experience overall reversed plastic straining in each cycle. Finally, the effect of crack closure on crack-growth driving force, especially that due to plasticity-induced crack closure, has yet to be clarified.

The objective of this study is to address the aforementioned issues by quantifying the interaction between fatigue cracks and elastic obstacles, with a view of developing a mechanistic model for microstructurally short cracks. The emphasis will be placed on the characterisation of crack-tip opening displacement and the plasticity-induced crack-closure of a crack approaching an elastic barrier, as shown in Figure 1(a), which represents an edge crack initiated in a surface crystal and growing towards the grain boundary. Two other configurations of engineering importance are also considered: a bi-material with an edge crack which is perpendicular to the interface, and a semi-infinite crack with a round elastic obstacle situated directly ahead of the crack tip. The first two cases are to simulate the blocking effect of grain boundaries on the growth of fatigue cracks, whereas the third configuration is representative of a crack growing towards a second phase particle or an inclusion in a material. Only the phase

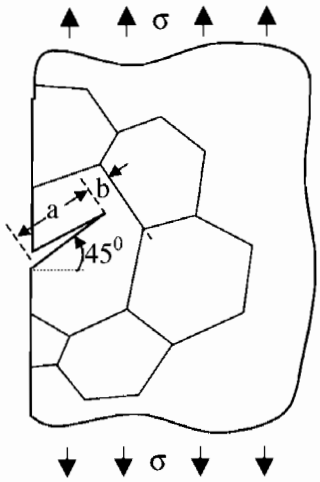


*Figure 1.* Edge crack emanating from a surface grain.

that contains the crack can deform plastically but both constituents have the same elastic properties.

Parametric solutions are obtained by elastic-plastic finite element analysis under monotonic (see Sections 2, 3, and 4) and cyclic loading conditions (see Sections 5 and 6), for both small-scale yielding and large scale yielding conditions. Where possible the present results are compared against the predictions of dislocation-based models and a simple double-slip model. It is worth noting that in the macro scale, deceleration has also been observed for long cracks approaching a bi-material interface perpendicularly from the weaker material, whose yield stress is lower than the material on the other side of the interface (Sugimura et al., 1995; Kim et al., 1997). So the present solutions will apply also to long cracks approaching bi-material interfaces.

## 2. Small-scale yielding solutions

Fatigue cracks, in polycrystalline alloys as well as single crystals, tend to initiate on slip plane facets at some oblique angle to the principal stress direction, as illustrated in Figure 1. Therefore microstructurally short cracks are often of mixed mode. For instance, the mode ratio of a crack inclined at 45 degrees to the loading axis is approximately $-0.5$ (Hutchinson and Tvergaard, 1999). Depending on the prevailing slip systems of the material, plastic flow at the crack tip may be confined to only one set of mutually orthogonal slip planes (Saeedvafa and Rice, 1992), or can occur along multiple sets of slip planes, i.e., unconstrained. Crack-tip plastic deformation can be further complicated by the width of the slip planes (Hutchinson and Tvergaard, 1999). In the present study we will limit our attention to the case of a mode I crack in a material whose plastic flow is not confined to a limited number of slip planes, i.e., the plastic deformation can be characterised by homogeneous plasticity theories. It is expected that the plastic deformation under mode II conditions can be well characterised using the dislocation-theory based block-slip models (Tanaka et al., 1986; Navarro and del los Rios, 1987, 1988) and hence will not be discussed here.

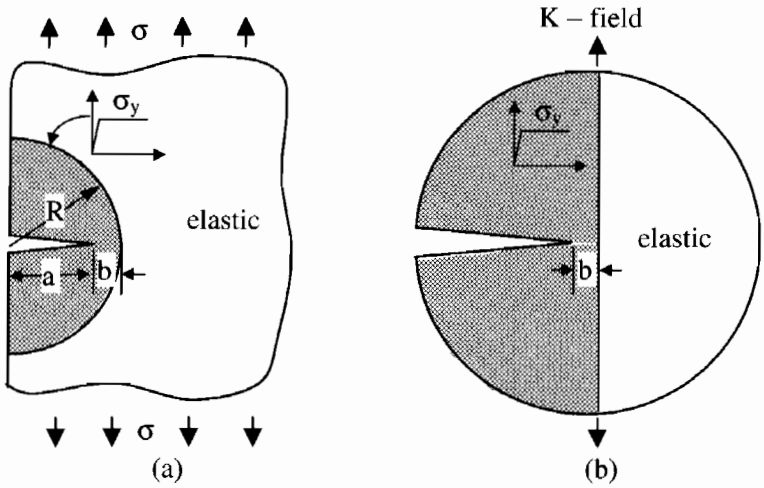


*Figure 2.* (a) A mode I crack growing in a semi-circular grain, and (b) a semi-infinite crack approaching an elastic barrier, representative of small-scale yielding conditions.

### 2.1. Finite element analysis

Consider the problem of an edge crack approaching an elastic barrier from within a semi-circular grain, as shown in Figure 2(a). Both materials possess identical elastic properties (Young's modulus $E$ and Poisson's ratio $\nu$) but only the grain within which the crack exists deform plastically, and therefore the problem can be viewed as elastically homogeneous but plastically inhomogeneous. The radius of the grain, the crack length and the distance between the crack tip and the barrier are denoted as $R$, $a$, and $b$, respectively. In this section we will focus on the small-scale yielding case where the plastic zone size is much smaller than the crack size and the distance $b$ is much less than the size of the singularity zone at the crack tip; large-scale yielding will be considered in the next section. In this case, the problem can be analysed by a small-scale yielding formulation, whereby the actual crack problem is replaced by a semi-infinite crack in an infinite body containing an elastic obstacle at distance $b$ away from the crack tip, as depicted in Figure 2(b). This problem is similar to that considered by Sugimura et al. (1995), who determined the $J$-integral using the finite element method.

The size of the plastic zone is of the order, ignoring the blocking effect of the elastic obstacle,

$$R = \left(\frac{K}{\sigma_Y}\right)^2, \tag{1}$$

where $K$ denotes the applied stress-intensity factor and $\sigma_Y$ the yield stress of the elastic-plastic material. This pertaining boundary-value problem, which has two independent length scales $b$ and $R$, can be analysed using a boundary layer approach (Rice, 1968; Willis, 1997). Relative to the length scale $R$, the crack appears to be semi-infinite, in an infinite body, subject to remote loading given by the following equation as $r/R \to \infty$,

$$\hat{\sigma}_{ij}\left(\hat{r}, \theta\right) = \frac{1}{\sqrt{2\pi\hat{r}}} f_{ij}\left(\theta\right) + \hat{T}\delta_{1i}\delta_{1j}, \tag{2}$$

where $(r, \theta)$ are polar coordinates centred at the crack tip. The symbol $\wedge$ is used to distinguish normalised parameters, i.e., $\hat{r} = r/R$, $\hat{\sigma}_{ij} = \sigma_{ij}/\sigma_0$, $\hat{T} = T/\sigma_Y$, and $\delta_{ij}$ is the Kronecker delta.

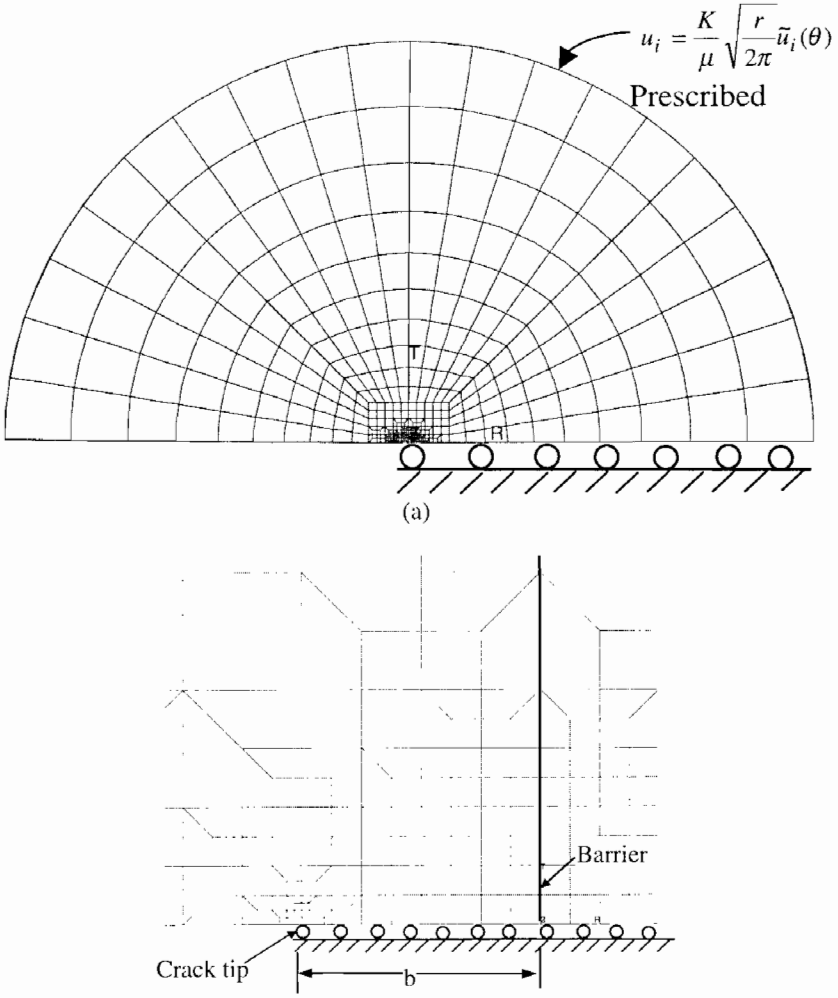


*Figure 3.* Finite element mesh for small-scale yielding condition, showing (a) boundary conditions, (b) fine mesh near a straight boundary.

Catalogues of results for stress intensity factors $K$, the functions $f_{ij}(\theta)$, and the constant term $T$ are available for a wide variety of crack geometries (e.g., Leevers and Radon, 1982). For convenience, the $K$-field is applied by imposing a displacement along the boundary of the finite element model,

$$\hat{u}_{ij}(\hat{r}, \theta) = \frac{\sqrt{\hat{r}}}{\sqrt{2\pi}} \frac{\sigma_Y}{E'} g_i(\theta, \nu) + \frac{\sigma_Y}{E'} \hat{r}\, \hat{T}\, h_i(\theta, \nu), \tag{3}$$

where $E'$ denotes the generalised Young's modulus ($E' = E$ for plane stress and $E' = E/(1-\nu^2)$ for plane strain). The angular functions $g_i$ and $h_i$ can be deduced from the known results by Williams (1957). The above displacements are applied to the boundary of the finite element model, as depicted in Figure 3. The finite element model is constructed using eight-noded, quadrilateral elements. To ensure the small-scale yielding condition, the strength of the applied $K$-field is chosen so that the plastic-zone size given by Equation (20) is less than one-tenth of the size of the finite element model.

Let us define the crack face opening displacement as $\delta$,

$$\delta(r) = u_y(r, \theta = \pi) - u_y(r, \theta = -\pi). \tag{4}$$

Close to the crack tip, e.g. $\hat{r} \ll 1$, the crack face displacement can be expressed as (Hutchinson and Tvergaard, 1999),

$$\hat{\delta} = \hat{\delta}_t + A\hat{r} - B\hat{r}\ln\hat{r}, \tag{5}$$

where $\hat{\delta}_t$ is the desired crack-tip opening displacement(CTOD). This provides a convenient method for determining the CTOD based on the displacement results obtained using a finite element analysis. It is noted that the above definition of CTOD ($= R\hat{\delta}_t$) differs slightly from the operational definition advocated by Rice and Tracy (1976), but is consistent with the classical Dugdale solution for plane stress condition. According to the Dugdale model, for a centre crack (with length of $a$) subjected to uniform stress ($\sigma$), the crack face opening displacement can be expressed as,

$$\delta(r) = \frac{8\sigma_Y a}{\pi E}\ln\frac{c}{a} + r\frac{4\sigma_Y}{\pi E}\ln\left[2\left(1 - \frac{a^2}{c^2}\right)\right] - \frac{4\sigma_Y}{\pi E}r\ln\frac{r}{a}, \tag{6}$$

where $c$ denotes the plastic zone size, which is given by $c = a/\cos(\pi\sigma/2\sigma_Y)$.

It can be shown that the normalised crack opening displacement behind the crack tip depends on three non-dimensional variables,

$$\hat{\delta} = \frac{\delta(r)}{R} = \hat{\delta}\left(\hat{r}; \hat{T}, \hat{b}\right), \tag{7}$$

where $\hat{b} = b/R$. Consequently, the normalised crack-tip opening displacement $\hat{\delta}_t$ defined in Equation (24) depends on only two non-dimensional parameters,

$$\hat{\delta}_t = \frac{\sigma_Y}{E'} f\left(\hat{T}, \hat{b}\right), \tag{8}$$

where the dimensionless function $f$ can be determined numerically using, for example, finite element methods. Therefore, the crack-tip opening displacement $\delta$ for a crack approaching an elastic obstacle can be expressed as,

$$\delta = R\hat{\delta}_t\left(\hat{T}, \hat{b}\right) \equiv f\left(\frac{T}{\sigma_Y}, \frac{b}{R}\right)\frac{K^2}{E'\sigma_Y}, \tag{9}$$

where the function $f$ can be computed using the finite element method for fixed $b$ with varying $R$ (through varying material's yield stress) or for fixed $R$ with varying $b$. In the special case of zero $T$-stress, the coefficient $f$ depends solely on the normalised distance $b/R_P$,

$$\delta = f_0\left(\frac{b}{R_P}\right)\frac{K^2}{E'\sigma_Y}, \quad T = 0, \tag{10}$$

where $R_P = \pi K^2/8\sigma_Y^2$ for plane stress and $R_P = K^2/3\pi\sigma_Y^2$ for plane strain. Solutions of the function $f_0$ will be determined in the following section.

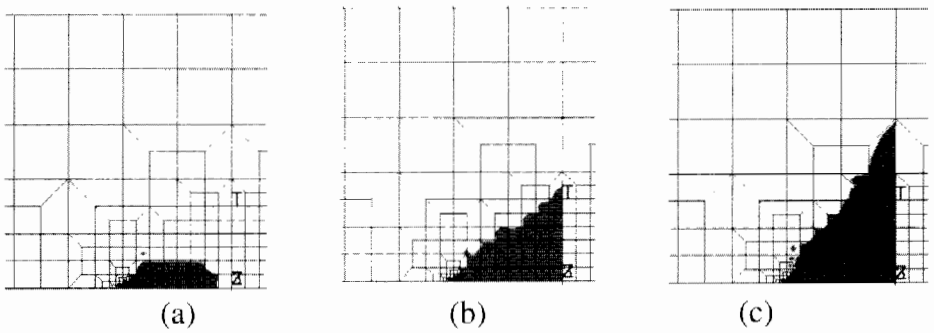


*Figure 4.* Contour of plastic zone (shaded area) under plane stress conditions: (a) $b/R_P = 1.1$, (b) $b/R_P = 0.327$, (c) $b/R_P = 0.247$.

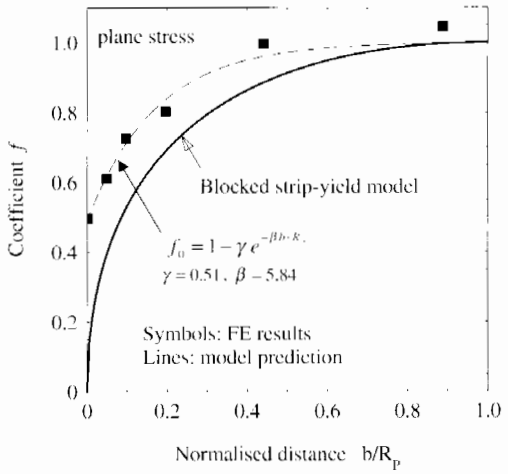


*Figure 5.* Solutions of coefficient $f_0$ under plane stress conditions.

## 2.2. Solutions for a crack approaching an elastic barrier

Under plane stress conditions, three typical contours of the plastic zone are displayed in Figure 4 (indicated by the shaded area). It is clear from Figure 4(a) that before the plastic zone reaches the barrier, plastic deformation concentrates in a narrow band directly ahead of the crack tip, consistent with the well-known plane stress solution under small-scale yielding conditions. Contact between the plastic zone and the barrier occurs for $b/R_P \approx 1.0$, as expected. After the plastic zone reaches the barrier, it then extends vertically along the interface because the material across the interface remains elastic, as shown in Figures 4(b) and (c).

The crack-tip opening displacement $\delta$ is determined from the finite element results via Equation (24). Plot of $f_0$ as function of $b/R_P$ is shown in Figure 5. Also shown in the figure are the predictions based on a blocked strip-yield model (Tanaka et al., 1986; Navarro and de los Rios, 1987, 1988) which will be discussed in more detail later. Perhaps the most significant finding of the present study is that the crack-tip opening displacement does not approach zero as expected from the blocked strip-yield model. The main reason for this difference is due to the plastic flow in the direction perpendicular to the crack plane, which signifies a dramatic change in the mode of plastic deformation brought about by the interaction with elastic barri-

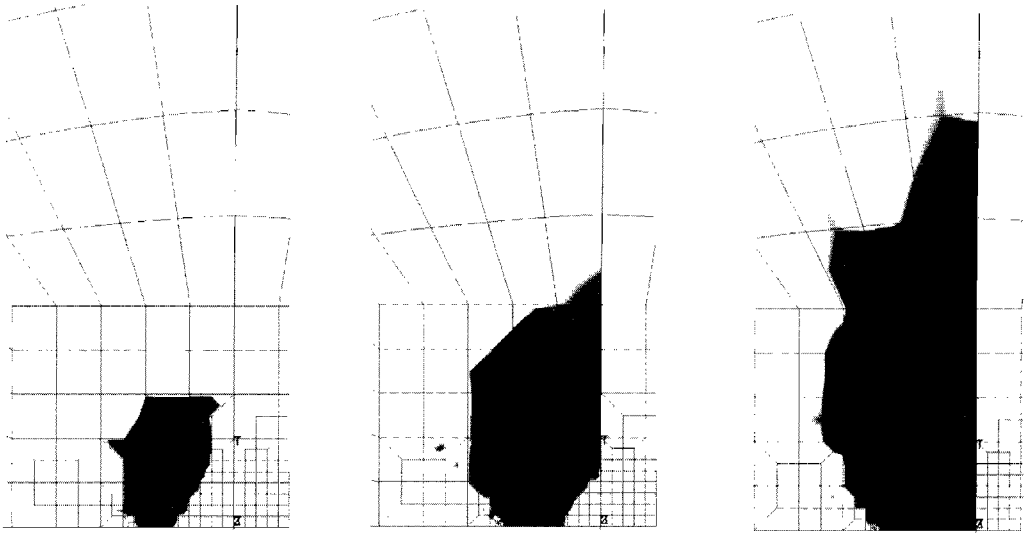


*Figure 6.* Contour of plastic zone (shaded area) under plane stress conditions: (a) $b/R_P = 0.693$, (b) $b/R_P = 0.39$, (c) $b/R_P = 0.25$.

ers. Therefore it is no longer appropriate to treat the plastic deformation as occurring within a narrow strip, even under plane stress conditions.

Figure 6 shows the evolution of the plastic zone under plane strain conditions. Before the plastic zone reaches the elastic barrier, the size of the plastic zone increases linearly with the square of the stress-intensity factor. Therefore, based on the results given in Figure 6(a), it can be calculated that the plastic zone extends to the barrier at $b/R_P \approx 0.52$, where $R_P = K^2/3\pi\sigma_Y^2$. As will become clear in the next section that this value is very close to that predicted by the blocked double-slip model. After the plastic zone reaches the barrier, it starts to extend vertically and along the interface, as shown in Figures 6(b) and (c). Two important observations can be made from the present results. First, before the plastic zone reaches the elastic barrier, the plastic flow at the crack tip tends to be more diffused under plane strain conditions than under plane stress conditions, implying that the double-slip model of Rice (1974) would be more appropriate for this case. Secondly, once the plastic zone reaches the elastic barrier, plastic flow starts to spread in the direction perpendicular to the crack plane, causing the crack tip to 'slide' open by the shearing action along the interface.

Plot of $f_0$ as a function of $b/R_P$ under plane strain conditions is shown by the symbols in Figure 7. Like under plane stress conditions, the crack-tip opening displacement asymptotes to a non-zero value as $b/R_P \to 0$, i.e. when the crack tip approaches the barrier. The finite element results can be well correlated with the following simple interpolating function,

$$f_0 = 0.564\left[1 - \gamma\, e^{-\beta\, b/R_P}\right], \tag{11}$$

where $\gamma = 0.24$ and $\beta = 13.3$. The present results suggest that as the crack tip approaches an elastic barrier, the crack-tip opening displacement decreases only by about 24% for plane strain, compared with a 51% reduction under plane stress conditions. The important implications of this non-zero limiting value in terms of to fatigue crack growth will be discussed later. For comparison purposes, predictions based on a blocked double-slip model (to be discussed later) are also plotted in Figure 7.

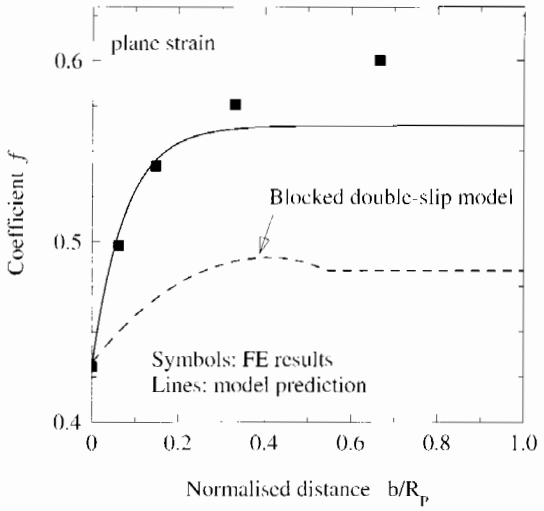


*Figure 7.* Normalized CTOD of a crack approaching an obstacle under plane strain conditions.

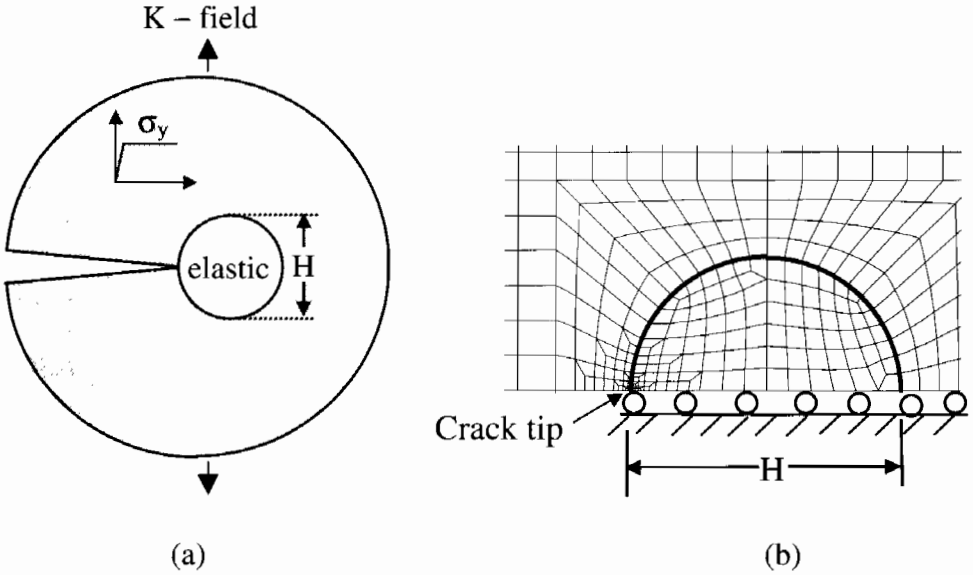


*Figure 8.* A semi-finite crack terminating at a round obstacle. (a) Geometry and (b) finite element mesh near crack tip.

## 2.3. Crack terminating at round obstacle

Another problem of practical engineering significance is the interaction between a fatigue crack and a brittle particle or an inclusion. Similar to the results presented in the previous section, the crack-tip opening displacement will attain the minimum value when the crack tip terminates at the obstacle, as illustrated in Figure 8(a). Here an ideal round obstacle will be considered, with the diameter of the round obstacle being denoted as $H$. It can be shown

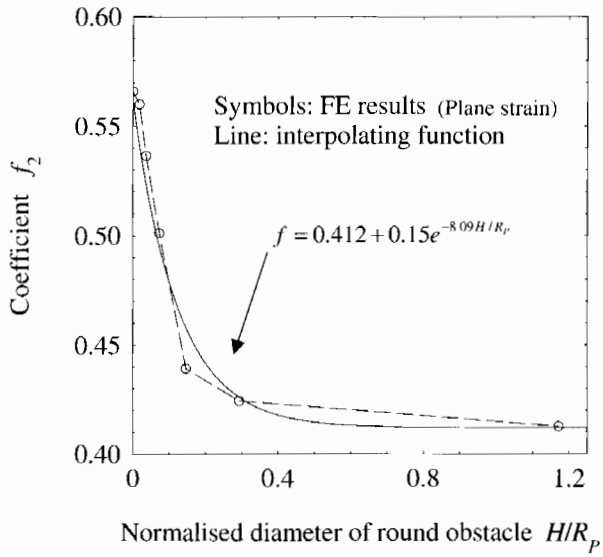


*Figure 9.* The coefficient specifying the crack-tip opening displacement for a crack approaching a round obstacle.

by a dimensional analysis that the crack-tip opening displacement depends on only one non-dimensional variable $H/R_P$,

$$\delta = f_2\left(\frac{H}{R_P}\right)\frac{K^2}{E'\sigma_Y}. \tag{12}$$

The parametric function $f_2$ will now be determined using the finite element method outlined in Section 2.1, except that the mesh near the crack tip is replaced by that shown in Figure 8(b).

Plot of $f_2$ as a function of $H/R_P$ is displayed in Figure 9, indicating that as the size of the obstacle increases the crack-tip opening displacement decreases sharply. The results suggest that a round obstacle is very effective in blocking the crack-growth driving force, with $f_2$ reaching the minimum value at $H/R_P = 0.5$. This implies that the maximum enhancement in fatigue crack growth resistance can be expected from brittle particles with a diameter equal to half the crack-tip plastic zone size, provided the particles are not fractured by the high stress level ahead of the advancing crack tip.

## 3. Blocked-slip models

In analysing the blocking effect of microstructural obstacles on the growth of short cracks, blocked-slip models have been developed for the crack-tip sliding and opening displacements which consider grain boundary blockage (Tanaka et al., 1986; Navarro and de los Rios, 1987, 1988; Wang, 1996). This type of model can qualitatively simulate the observed deceleration/acceleration in fatigue crack growth rates as the crack grows through periodic obstacles. Nevertheless, it should be pointed out that these models have been developed for shear mode cracking and later extended to tensile mode crack growth by appealing to the Dugdale model for plane stress, i.e., plastic deformation is assumed to occur within a narrow strip ahead of the crack tip. The results displayed in Figure 4 clearly suggest that such an idealisation is over simplified and does not reflect the lateral expansion of the plastic zone. To further elucidate

this point, it is insightful to examine the behaviour of the blocked strip-yield model, with a view of circumventing the deficiencies. To this end, the blocked strip-yield model is first assessed and then an extension of Rice's double-slip model is proposed to account for the interaction of a plane strain crack with an elastic barrier.

### 3.1. Blocked strip-yield model for plane stress

The essence of the blocked strip-yield model (Tanaka et al., 1986; Navarro and de los Rios, 1987, 1988) is to represent the crack and the plastic zone, which is assumed to be an infinitely thin strip, by distributed dislocations with the Burgers vectors parallel (for shear mode) or perpendicular (for tensile mode) to the crack plane. The equilibrium equation determining the dislocation distributions is identical to the standard Dugdale model in the form of the Cauchy type of singular integral equation. However, due to the blocking of the barrier, plastic deformation is not fully relaxed. Instead there is a stress singularity at the point where the plastic zone intersects the barrier. In this case, the dislocation distribution is given by the unbounded solution of the integral equation (Navarro and de los Rios, 1987), from which the crack-tip opening displacement can be determined. For the particular case of small-scale yielding, the following expression can be obtained, omitting the details of derivation,

$$\delta = \left[ 2\sqrt{\frac{b}{R_P}} - \frac{b}{R_P} \right] \frac{K^2}{E\sigma_Y}, \qquad (b \leq R_P), \tag{13}$$

which recovers the standard Dugdale solution when $b = R_P$. It is clear that the blocked strip yield model predicts $\delta \to 0$ as $b/R_P \to 0$. However, the finite element results, as shown in Figure 5, suggest that

$$\delta \to 0.49 \frac{K^2}{E\sigma_Y} \qquad \text{as} \qquad b/R_P \to 0.$$

This large difference between the computational results and the blocked strip-yield model in the small $b/R_P$ limit is essentially due to the overly simple idealisation of plasticity occurring within a strip, which is obviously inconsistent with the finite element solution shown in Figure 4. Therefore the assumption of strip yielding needs to be abandoned if an improved analytical model is to be developed. This will be the subject of future work.

### 3.2. Blocked double-slip model for plane strain

As shown in Figure 6, the plastic deformation under plane strain conditions tends to concentrate within bands inclined at an angle to the crack plane, lending support to the double-slip model developed by Rice (1974). The double-slip model assumes that plastic relaxation occurs by sliding on two bands at angles $\pm\phi$ with the crack plane. These bands sustain a yield stress $\tau_0 = \sigma_Y/\sqrt{3}$ in shear, whose length is given by (Rice, 1974)

$$r_P(\phi) = \frac{3\pi}{64} \sin^2\phi \, [1 + \cos\phi] \, \frac{K^2}{\sigma_Y^2}. \tag{14}$$

The crack-tip sliding displacement is

$$\delta_t^{(s)} = \frac{\sqrt{3}}{8} \sin^2\phi \, [1 + \cos\phi] \, \frac{K^2}{E'\sigma_Y}. \tag{15}$$

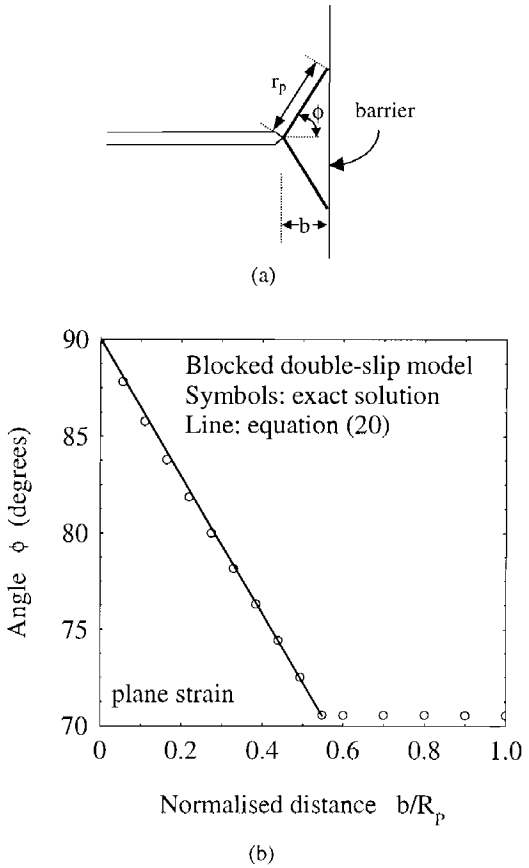


*Figure 10.* Blocked double-slip model, showing (a) geometry and (b) angle of the slip bands.

Hence the crack-tip opening displacement CTOD can be expressed as

$$\delta \approx 2\delta_t^{(s)} \sin\phi = \frac{\sqrt{3}}{4} \sin^3\phi \,[1 + \cos\phi] \frac{K^2}{E'\sigma_Y}. \tag{16}$$

In the absence of an elastic barrier Rice (1974) showed that the inclination angle $\phi$ is that which maximises the extent of the plastic zone, $\partial r_P/\partial\phi = 0$, leading to $\phi_0 = cos^{-1}\frac{1}{3} \approx 70.53°$. For a given applied stress-intensity factor, the distance $b$ at which the plastic zone just reaches the interface can be readily determined,

$$b_0 = r_p(\phi_0)\cos\phi_0 = \frac{\pi^2}{18} R_P, \tag{17}$$

where $R_P = K^2/3\pi\sigma_Y^2$. This gives $b_0/R_P = 0.548$, which is very close to that determined using the finite element method $b/R_P \approx 0.52$ (see Section 2.2).

When the plastic zone interacts with the elastic barrier, the blocking action of the barrier means that the plastic relaxation cannot occur in the optimum direction $\phi_0$, instead, the following geometrical relation must hold,

$$r_p(\phi)\cos\phi = b, \qquad \left(b/R_P \le \pi^2/18\right). \tag{18}$$

Now the angle $\phi\,(b/R_P)$ can be determined by solving the above equation. The results are plotted in Figure 10, which reveals that the angle $\phi$ varies almost linearly with $b/R_P$, and hence can be well approximated by the following expression,

$$\phi = \frac{\pi}{2} - \frac{18}{\pi^2}\left(\frac{\pi}{2} - \phi_0\right)\frac{b}{R_P}, \qquad (b/R_P \leq \pi^2/18). \tag{19}$$

With the angle $\phi$ given by the above expression, the crack-tip opening displacement can be readily computed using Equation (16) and the results are plotted in Figure 7. These results indicate that in the small $b/R_P$ limit, predictions of the blocked double-slip model are in close agreement with the finite element results, but not for large $b/R_P$ values. This is to some extent due to the simplified representation of the plastic deformation by plastic shearing along two bands of zero thickness. The actual plastic deformation under plane strain condition, as shown in Figure 6, tends to diffuse over a large area, especially before the plastic zone reaches the barrier.

## 4. Large-scale-yielding solutions

In the preceding analysis it has been assumed that small-scale yielding, at least at the scale of the microstructure, would prevail. However, for fatigue cracks to initiate in a polycrystal without stress concentrators, the applied stress generally exceeds the limit of small-scale yielding. Therefore it is important to extend the above analysis to consider stage I crack experiencing large-scale or even gross-section yielding. For simplicity, the case of a centre crack in an infinite, homogeneous, material will be considered first. The CTOD results for plane strain are plotted in Figure 11(a), together with the calculations based on the modified Dugdale model (Equation (6)) where the yield stress is replaced by $\alpha\sigma_Y$. Here the parameter $\alpha$ denotes the plasticity constraint factor for plane strain deformation (Newman, 1998). The reason for the underestimation of the crack-tip opening displacement by the modified Dugdale model is primarily due to the loss of plastic constraint associated with large-scale yielding. A simple interpolating function can be constructed to correlate the computational results,

$$\delta_\infty = 0.564\frac{K^2}{E\sigma_Y}\left[1 + A\frac{\sigma}{\sigma_Y}\right], \tag{20}$$

where $A = 0.758$. Here the subscript $\infty$ is used to denote the CTOD solution for a crack far removed from any elastic barrier. This result will be employed later to determine the dependence of fatigue limit on crack length.

Consider the case of a crack embedded in an elastic-plastic grain surrounded by an elastic domain, as shown in Figure 2(a), with the applied stress approaching or exceeding the yield stress of the grain that contains the crack. Since the crack-tip opening displacement will decrease as the crack tip approaches the grain boundary, the most significant case in terms of continuous growth or crack arrest is the condition when the crack tip reaches the barrier. In the following attention will be restricted to this limiting case. It can be shown by dimensional analysis that the crack-tip opening displacement can be expressed in the following non-dimensional form,

$$\delta_0 = a\varepsilon_0 g\left(\frac{\varepsilon}{\varepsilon_0}\right), \tag{21}$$

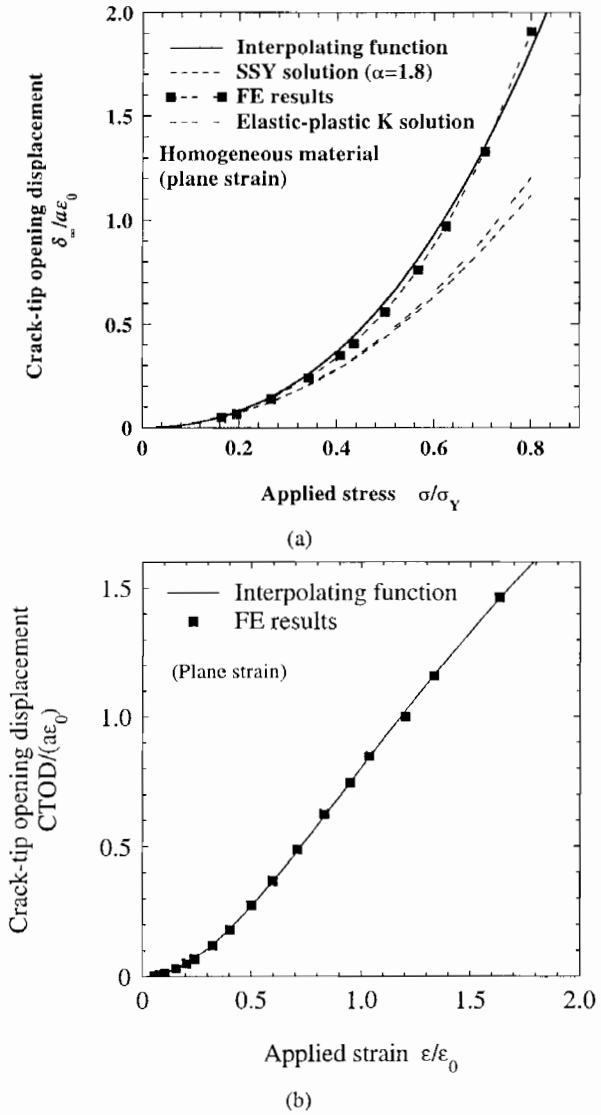


*Figure 11.* Large-scale yielding solutions of the CTOD for (a) an edge crack in a homogeneous material and (b) an edge crack with its tip terminating at an elastic barrier.

where $\varepsilon_0 = \sigma_Y/E$ and the function $g$ needs to be determined by computational methods. The results of the finite element analysis under plane strain conditions are shown in Figure 11(b). It can be seen that at low stress, $\sigma/\sigma_Y \ll 1$, the crack-tip opening displacement scales with the square of the applied strain (or stress). At high stress, however, CTOD tends to increase almost linearly to the applied strain. Based on the finite element solution the following interpolating function can be constructed,

$$\delta_0 = f_0(0)\,\pi a\varepsilon_0 \frac{(\varepsilon/\varepsilon_0)^2}{1 + B\,(\varepsilon/\varepsilon_0)^m} = \frac{f_0(0)}{1 + B\,(\varepsilon/\varepsilon_0)^m}\frac{K^2}{E\sigma_Y}, \qquad \text{for} \quad \sigma \le \sigma_Y, \tag{22}$$

where $B = 0.604$, $m = 1.65$, and $f_0(0)$ is given by Equation (11), i.e., $f_0(0) = 0.428$, which is consistent with the small-scale yielding solutions.

## 5. Plasticity induced fatigue crack closure

The preceding results can be extended to cyclic loading, provided that crack faces do not come into contact during the load cycle. However, fatigue crack closure, especially that induced by the plastic wake left behind by an advancing crack, occurs even when the minimum stress in a loading cycle is tensile (Elber, 1970). The concept of crack closure is critical to rationalising almost every aspect of fatigue crack growth, such as the mean stress effect and the sequence effect associated with spectrum loading. It is worth recalling two important results regarding plasticity-induced crack closure. Under constant $K$-loading, Budiansky and Hutchinson (1978) presented an elegant solution for the problem of *steady-state* crack closure, where the residual plastic wake behind the advancing crack tip is of constant thickness. For a crack growing under constant amplitude load, however, the plastic wake thickness increases linearly with increasing crack length, giving rise to *self-similar* crack closure (Wang and Rose, 1999b; Rose and Wang, 1999). The results presented in Section 3 highlight two important differences between a crack in a homogeneous material and a crack advancing towards an elastic barrier. First, the crack-tip opening displacement decreases as the crack tip approaches the barrier, indicating that the plastic wake thickness would decrease with increasing crack length. Secondly, the mode of plastic flow changes dramatically due to the interactions with barriers, as displayed in Figure 6. Therefore, it is important to quantify how the interactions with elastic obstacles will affect the plasticity-induced crack closure.

In the present study the crack closure behaviour is analysed by the finite element method, which involves introducing two sets of bi-linear spring-elements along the crack plane. One set of springs, which have zero stiffness in tension and infinite stiffness in compression, are attached to all the nodes along the crack plane (ahead as well as behind of the crack tip) to prevent crack faces from overlapping under compression. Another series of tension-only spring elements, which have infinite stiffness in tension and zero stiffness in compression, are attached to the nodes ahead of the crack tip to maintain the zero displacement condition under tension. To quantify the effect of plasticity-induced crack closure, the finite element model is subjected to a cyclic load while one tension-only spring element is released (hence crack grows by element width) after every two cycles. The crack-closure stress ($\sigma_{cl}$) and the crack-opening stress ($\sigma_{op}$) are defined as the stresses at which contact or separation occurs at the nodes immediately behind the crack tip. Plots of the crack-closure stress $\sigma_{cl}$ are shown in Figure 12. It is clear that the crack-closure stress increases as the crack tip approaches the elastic obstacle. Due to crack face closure, the cyclic crack-tip opening displacement $\Delta\delta$, which is dictated by the effective stress range $\Delta\sigma = \sigma_{\max} - \sigma_{cl}$, will decrease even faster than the maximum CTOD as the crack tip approaches the obstacle. The rapid reduction in $\Delta\delta$ implies that fatigue crack-growth rates will decrease sharply as the crack tip grows towards the barrier, consistent with some experimental observations (Sugimura et al., 1995).

In the case of small-scale yielding conditions, $\Delta\delta$ can be readily determined from equations (10), provided that $K$ is replaced by $\Delta K_{\text{eff}}$ (Budiansky and Hutchinson, 1978),

$$\Delta\delta = f_0\left(\frac{b}{R_{P,c}}\right)\frac{\Delta K_{\text{eff}}^2}{2E'\sigma_Y}, \tag{23}$$

where $\Delta K_{\text{eff}} = U \cdot \Delta K$, the function $f_0$ is given by Equation (11) and $R_{P,c}$ denotes the cyclic plastic zone size,

$$R_{P,c} = \frac{1}{3\pi}\left(\frac{\Delta K_{\text{eff}}}{2\sigma_Y}\right)^2. \tag{24}$$

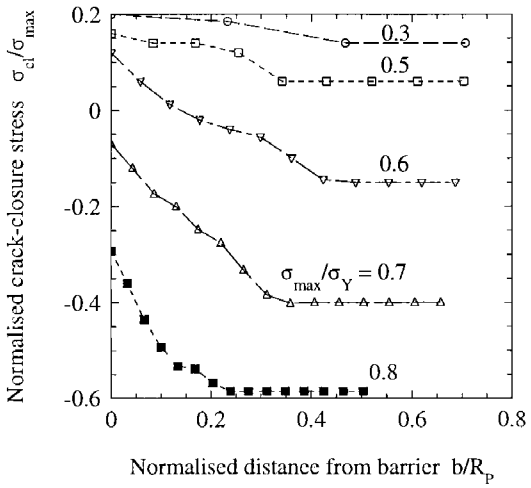


*Figure 12.* Crack-closure stress for an edge crack approaching an elastic barrier.

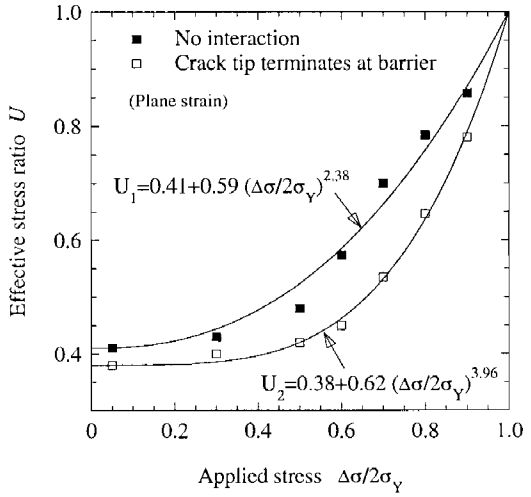


*Figure 13.* Effective stress ratio $U$ for an edge crack in a homogeneous solid and an edge crack terminating at an elastic barrier.

Here the effective stress ratio $U$ is defined as,

$$U = \frac{\sigma_{\max} - \sigma_{cl}}{\sigma_{\max} - \sigma_{\min}}. \tag{25}$$

Under large-scale yielding, the cyclic crack-tip opening displacement $\Delta\delta$ can be determined by a similar method from Equations (22) or (20) provided that $\sigma$ is replaced by $U\cdot\Delta\sigma$, and $\sigma_Y$ is replaced by $2\sigma_Y$. Under fully reversed loading, i.e., $R = -1$, the effective stress ratio $U$ depends on only one non-dimensional parameter $\Delta\sigma/2\sigma_Y$. Figure 13 shows the finite element solution of $U$ for various stress ratios, which can be correlated by the following equation,

$$U_1 = C_1 + (1 - C_1)\left(\frac{\Delta\sigma}{2\sigma_Y}\right)^{C_2}, \tag{26}$$

with $C_1 = 0.41$, $C_2 = 2.38$ for the case of no interaction between the crack-tip plastic zone and the elastic barrier,

$$U_2 = C_3 + (1 - C_3)\left(\frac{\Delta\sigma}{2\sigma_Y}\right)^{C_4} \tag{27}$$

and $C_3 = 0.38$, $C_4 = 3.96$ for the case when the crack tip terminates at the barrier.

## 6. Fatigue limit and threshold of small fatigue cracks

With the merging of fatigue and fracture mechanics approaches (Newman, 1998), fatigue limit is now considered to be synonymous with fatigue crack growth threshold (Miller, 1993a), provided the effects of large-scale yielding or gross-section yielding experienced by small cracks are adequately taken into account. A key requirement to a rigorous mechanistic approach to analyse the large-scale yielding behaviour of small fatigue cracks is a suitable correlating parameter which can establish a similitude between short and long cracks (Wang and Rose, 1999a). In the present study, let us adopt the cyclic crack-tip opening displacement as the correlating parameter, and the growth rate follows a general relation,

$$\frac{\mathrm{d}a}{\mathrm{d}N} = h\left(\Delta\delta, \Delta\delta_{th}\right), \tag{28}$$

where $\Delta\delta_{th}$ represents a threshold value which may depend on environment and temperature for a given material. This threshold value may be due to intrinsic material resistance or crack surface roughness, both are not considered in analysing the plasticity-induced crack closure. For a given material, the function $h$ can be determined using standard specimens.

The present results reveal that as the crack approaches a microstructural barrier, the cyclic crack-tip opening displacement $\Delta\delta$ decreases, whereas the stress concentration at the barrier increases. Therefore the fatigue limit of a polycrystalline material could be related to the stress below which (i) the $\Delta\delta$ is less that the threshold value $\Delta\delta_{th}$, and (ii) the crack is unable to initiate new slip across the microstructural barrier. Therefore determination of the fatigue limit of a component containing a crack of length $a$ requires solving a set of coupled equations representing the aforementioned conditions. However, two bounds on the fatigue limit stress range $\Delta\sigma_{FL}$ can be obtained assuming that the fatigue limit corresponds to (1) the onset of interaction and (2) crack tip terminating at the barrier ($h = 0$), respectively. These two bounds will be termed as Model 1 and Model 2. As will be seen later, the two bounds are virtually the same for medium applied stress $\Delta\sigma_{FL}/2\sigma_Y \leq 0.7$.

Under fully reversed loading ($R = -1$), the lower bound can be mathematically expressed as,

$$\delta_\infty\left(U_1\Delta\sigma_{FL}/2\sigma_Y\right) = 0.564\frac{\left[\Delta K_{th\infty}U_1(0)\right]^2}{2E\sigma_Y}, \tag{29}$$

where the function $\delta_\infty$ is given by Equation (20) and $U_1$ is given by Equation (26). In particular, $U_1(0) = C_1 = 0.41$. Then the stress-intensity factor threshold is be related to the stress level at which the threshold value is measured via the following equation,

$$\frac{\Delta K_{th}}{\Delta K_{th\infty}} = \frac{U_1(0)}{U_1}\frac{1}{\sqrt{1 + A \cdot U_1 \cdot \Delta\sigma_{FL}/2\sigma_Y}}, \tag{30}$$

ratio on the cyclic crack-tip opening displacement, which will allow further unification of experimental data obtained under various mean stresses.

## 7. Conclusions

Basic solutions of the crack-tip opening displacement and the plasticity-induced crack closure for a mode I fatigue crack growing towards elastic obstacles have been determined using an elastic-plastic finite element method. The results show that for a given applied load the crack-tip opening displacement decreases as the crack-tip approaches the interface boundary, but reaching a non-zero value when the crack tip reaches the barrier. Under fully reversed cyclic loading, the plasticity-induced crack closure has been found to increase as the crack grows towards the barrier. A mechanistic model is proposed to relate the fatigue threshold of microstructurally small fatigue cracks to the cyclic crack-tip opening displacement reaching a critical value. Predictions of the model correlate reasonably well with experimental data.

## Acknowledgements

This work was supported in part by the Australian Academy of Science through the provision of Scientific Visit Award to one of the authors (C.H. Wang). The authors would like to thank Prof. S. Suresh and Dr L.R.F. Rose for helpful discussions.

## References

Budiansky, B. and Hutchinson, J.W. (1978). Analysis of closure in fatigue crack growth. *Journal of Applied Mechanics* **45**, 267–275.

Elber, W. (1970). Fatigue crack closure under cyclic tension. *Engineering Fracture Mechanics* **2**, 37–45.

Haddad, M.H. El, Smith, K.N. and Topper, T.H. (1979). Fatigue crack propagation of short cracks. *Journal of Engineering Materials and Technology* **101**, 42–46.

Hutchinson, J.W. and Tvergaard, V. (1999). Edge-cracks in single crystals under monotonic and cyclic loads. *International Journal of Fracture* **99**, 81–95.

Kim, A.S., Suresh, S. and Shih, C.F. (1997). Plasticity effects on fracture normal to the interfaces with homogeneous and graded compositions. *International Journal of Solids and Structures* **34**, 3415–3432.

Leevers, P.S. and Radon, J.C. (1982). Inherent stress biaxiality in various fracture specimen geometries. *International Journal of Fracture* **19**, 311–325.

Liu, H.W. (1998). A dislocation barrier model for fatigue crack growth threshold. *International Journal of Fracture* **93**, 261–280.

McDowell, D.L. (1996). Basic issues in the mechanics of high cycle metal fatigue. *International Journal of Fracture* **80**, 103–145.

Miller, K.J. (1991). Metal fatigue – past, current and future. *Proceedings Institution of Mechanical Engineers* **205**, 1–14.

Miller, K.J. (1993a). The two thresholds of fatigue behaviour. *Fatigue and Fracture of Engineering Materials and Structures* **16**, 931–999.

Miller, K.J. (1993b). Materials science perspective of metal fatigue resistance. *Materials Science and Technology* **9**, 453–462.

Navarro, A. and de los Rios, E.R. (1987). A model for short fatigue crack propagation with an interpretation of the short-long crack transition. *Fatigue and Fracture of Engineering Materials and Structures* **10**, 169–186.

Navarro, A. and de los Rios, E.R. (1988). An alternative model of the blocking of dislocations at grain boundaries. *Philosophical Magazine* **A57**, 37–42.

Newman, J.C. (1998). The merging of fatigue and fracture mechanics concepts: a historical perspective. *Progress in Aerospace Sciences* **34**, 347–390.

Rice, J.R. (1974). Limitations to the small scale yielding approximation for crack tip plasticity. *The Journal of Mechanics and Physics of Solids* **22**, 17–26.

Rose, L.R.F. and Wang, C.H. (2001). Self-similar analysis of plasticity-induced closure of small fatigue cracks. *The Journal of Mechanics and Physics of Solids* **49**, 401–429.

Saeedvafa, M. and Rice, J.R. (1992). Crack tip fields in a material with three independent slip systems: NiAl single crystal. *Modelling and Simulation in Material Science and Engineering* **1**, 53–71.

Sugimura, Y., Lim, P.G., Shih, C.F. and Suresh, S. (1995). Fracture normal to a bimaterial interface: effects of plasticity on crack-tip shielding and amplification. *Acta Metallurgica Materials* **43**, 1157–1169.

Tanaka, K. (1987). Mechanisms and mechanics of short fatigue crack propagation. *JSME International Journal* **30**, 1–13.

Tanaka, K., Akiniwa, Y., Nakai, Y. and Wei, R.P. (1986). Modelling of small fatigue crack growth interacting with grain boundary. *Engineering Fatugue Mechanics* **24**, 803–819.

Tracey, D.M. (1976). Finite element solutions for crack-tip behaviour in small-scale yielding. *Journal of Engineering Materials and Technology* **98**, 146–151.

Wang, C.H and Miller, K.J. (1992). The effects of mean shear stress on short fatigue crack growth. *Fatigue and Fracture Engineering Materials and Structures* **15**, 1223–1236.

Wang, C.H. (1996). Short fatigue crack growth under asymmetrical loading. *Journal of Engineering Materials and Technology* **118**, 362–366.

Wang, C.H. and Rose, L.R.F. (1999a). Crack-tip plastic blunting under gross-section yielding and implications for short crack growth. *Fatigue and Fracture of Engineering Materials and Structures* **22**, 761–773.

Wang, C.H. and Rose, L.R.F. (1999b). Self-similarity of the plastic wake of short fatigue cracks. *Proceedings of International Workshop on Fracture Mechanics and Advanced Engineering Materials*. University of Sydney, Australia, 20–27.

Williams, M.L. (1957). On the stress distribution at the base of a stationary crack. *Journal of Applied Mechanics*, **24**, 111–114.